

**Paper No. 00-1134**

**REQUIREMENTS FOR EVALUATING TRAFFIC SIGNAL CONTROL  
IMPACTS ON ENERGY AND EMISSIONS BASED ON INSTANTANEOUS  
SPEED AND ACCELERATION MEASUREMENTS**

**Hesham Rakha**

Center for Transportation Research  
Virginia Polytechnic Institute and State University  
1700 Kraft Drive, Suite 2000 (0536)  
Blacksburg, VA 24061  
Phone: 540/231-2261 - Fax (540) 231-5214  
E-mail: rakha@ctr.vt.edu

**Michel Van Aerde \***

Center for Transportation Research  
Virginia Polytechnic Institute and State University

\* Deceased August 17, 1999

**K. Ahn**

Center for Transportation Research  
Virginia Polytechnic Institute and State University  
E-mail: kahn@vt.edu

**Antonio A. Trani**

Department of Civil and Environmental Engineering  
Virginia Polytechnic Institute and State University  
E-mail: vuel@vt.edu

**Transportation Research Board  
79<sup>th</sup> Annual Meeting  
January 9-13, 2000  
Washington, D.C.**

### ABSTRACT

The evaluation of many transportation network improvements is commonly conducted by first estimating average speeds from a transportation/traffic model and then converting these average speeds into emission estimates based on an environmental model such as MOBILE (EPA, 1993a). Unfortunately, recent research has shown that certainly average speed, and perhaps even simple estimates of the amount of delay and the number of stops on a link, are insufficient measures to fully capture the impact of ITS strategies such as traffic signal coordination. Specifically, it has been shown that for the same average speed, one can observe widely different instantaneous speed and acceleration profiles, each resulting in very different fuel consumption and emission levels. In attempt to address this limitation, this paper illustrates the application of a series of multi-variate fuel consumption and emission prediction models, both within a traffic simulation model of a signalized arterial, and directly to instantaneous speed and acceleration data from floating cars traveling down a similar signalized arterial.

The paper illustrates the application of these multi-variate relationships for eight light duty vehicles, ranging in size from subcompacts to mini-vans and sport utilities. These relationships were developed based on initial data obtained from an experimental study by the Oak Ridge National Lab (ORNL) (West *et. al.*, 1997). However, it is shown elsewhere that the same modeling structure can also effectively deal with similar relationships for high emitters, heavy-duty vehicles and cold starts. Prediction models to such new data from ORNL and Environmental Protection Agency (EPA) is currently being fit using the same statistical models. The objective of the paper is, therefore, to illustrate that the application of these instantaneous models is both feasible and practical, and that it produces results that are reasonable in terms of both their absolute magnitude and their relative trends. The application of these relationships to floating-car Global Positioning System (GPS) data are presented elsewhere.

The research reported in this paper is one step in a more comprehensive modeling framework for dealing with the impacts of Intelligent Transportation Systems on energy consumption and vehicle emissions. Other earlier steps include analyses of traffic diversion and induced demand, while latter steps include the independent validation of the estimated fuel consumption and emission estimates using direct on-road measurements. The ability to estimate fuel and emissions levels as a function of instantaneous speed and acceleration, in a consistent fashion for both field data and simulated data is, however, critical to the core of the overall framework.

## INTRODUCTION

With the introduction of Intelligent Transportation Systems (ITS), there is a need to evaluate and compare alternative ITS and non-ITS investments. In comparing alternatives, typically a number of Measures of Effectiveness (MOEs) are considered including vehicle delay, vehicle stops, vehicle fuel consumption, vehicle emissions, and accident risk. The assessment of the fuel consumption and emission impacts of alternative investments requires a highly sophisticated evaluation tool in order to capture both the microscopic dynamics of vehicle-to-vehicle and vehicle-to-control interaction, in addition to modeling vehicle fuel consumption and emissions that are sensitive to these vehicle dynamics.

Consequently, the assessment of the energy and emission impacts of alternative investments can be viewed as a two-level process. At the first level, the microscopic dynamics of traffic including car-following, lane changing, and acceleration/deceleration behavior need to be captured. The car-following models, together with the lane changing models, capture the steady-state behavior of traffic (no acceleration or deceleration), while the acceleration and deceleration models capture the transition behavior between steady states (non-steady state). At the second level, the energy and emissions of hydrocarbons (HC), carbon monoxide (CO) and oxides of nitrogen (NO<sub>x</sub>) need to be computed based on the instantaneous speed and acceleration estimates that were computed in the first level.

The objective of this paper is to demonstrate how the combination of these two integrated processes (microscopic vehicle dynamic model, and energy and emission model) can be utilized to evaluate alternative ITS initiatives. Specifically, this paper demonstrates the feasibility of the proposed approach using traffic signal control examples. These examples are presented in order to demonstrate the feasibility of the concept rather than to present specific results. Furthermore, the paper also briefly demonstrates the feasibility of applying the microscopic fuel consumption and emission models directly to field speed and acceleration data. It should be noted that a more extensive application of the fuel consumption and emission models to field Global Positioning System (GPS) data and its application within a microscopic simulation environment is beyond the scope of the paper, however it is presented elsewhere (Rakha *et al.*, 2000).

In terms of the layout of the paper, the first section briefly describes the vehicle dynamics model that is incorporated within the INTEGRATION microscopic simulation and assignment model. After describing the vehicle dynamics model, the following section describes how the energy and emission models were developed using data that were collected at ORNL. In addition, the section describes how the energy and emission models were incorporated within the INTEGRATION model in order to combine vehicle dynamics with vehicle energy and emissions. The following section performs a preliminary validation of the combined dynamic vehicle model and the energy and emission model using a very simple network under varying traffic conditions. The following section applies the microscopic fuel consumption and emission model to field data in order to demonstrate the potential of applying the model directly to field data and to make some preliminary comparisons between field and simulated speed and acceleration data. Finally, the conclusions of the study together with recommendations for further work are presented.

## VEHICLE DYNAMICS MODEL

As described earlier, this paper demonstrates how the combined use of a vehicle dynamic model in conjunction with an energy and emission model can serve as an evaluation tool for quantifying the environmental impacts of ITS and non-ITS deployments. Specifically, the approach described in this paper utilizes the INTEGRATION microscopic traffic assignment and simulation model as its vehicle dynamics model (Van Aerde and Yagar, 1988a and 1988b; Van Aerde *et al.*, 1996). The INTEGRATION model, which was developed over the past decade, has not only been validated against standard traffic flow theory (e.g. Rakha and Van Aerde, 1996), but has also been applied to real-life problems (e.g. Rakha *et al.*, 1998). This section provides a brief description of the INTEGRATION model in order to provide the reader with a basic understanding of the vehicle dynamics model that was utilized in the analysis presented in this paper.

The following section describes how energy and emission models were developed using field data, and how these models were incorporated within the INTEGRATION model in order to provide a unique evaluation tool.

The manner in which the INTEGRATION model represents traffic flow can be best presented by discussing how a typical vehicle initiates its trip, selects its speed, changes lanes, transitions from link to link, and also selects its route.

### **Initiation of Vehicle Trips**

Prior to initiating the actual simulation logic, the individual vehicles that are to be loaded onto the network need to be generated. As most available O-D (Origin-Destination) information is macroscopic in nature, INTEGRATION permits the traffic demand to be specified as a time series histogram of O-D departure rates for each possible O-D pair within the entire network. The actual generation of individual vehicles occurs in such a fashion as to satisfy the time-varying macroscopic departure rates that were specified by the modeler within the model's input data files. It can be noted that the model simply disaggregates an externally specified time-varying O-D demand matrix into a series of individual vehicle departures prior to the start of the simulation. These departure rates can be fully random (negative exponential time headway distribution), fully uniform, or partially uniform and random.

It should be noted that as the externally-specified demand file is disaggregated, each of the individual vehicle departures is tagged with its desired departure time, trip origin, and trip destination, as well as a unique vehicle number. This unique vehicle number can subsequently be utilized to trace a particular vehicle along the entire path towards its ultimate destination. It can also be utilized to verify that subsequent turning movements of vehicles at, for example, network diverges are assigned in accordance to the actual vehicle destinations, rather than some arbitrary turning movement probabilities, as is the case in many other microscopic models that are not assignment-based.

### **Determination of Vehicle Speed**

When the simulation clock reaches a particular vehicle's scheduled departure time, an attempt is made to enter that vehicle into the network at its origin zone. From this point, the vehicle will begin to proceed, in a link-by-link fashion, towards its final destination. Upon entering this first link, the vehicle will then select the particular lane in which to enter. This is usually the lane with the greatest available distance headway at the point of entry.

Once the vehicle has selected which lane to enter, the vehicle computes its desired speed on the basis of the distance headway between it and the vehicle immediately downstream of it, but within the same lane. This computation is based on a link-specific microscopic car-following relationship that is calibrated macroscopically to yield the appropriate target aggregate speed-flow attributes for that particular link (Van Aerde, 1995; Van Aerde and Rakha, 1995). The car-following model has been modified to also include the difference in speed between the vehicle and the vehicle immediately downstream of it. The details of the car-following model are beyond the scope of this paper, however, it is sufficient to mention that the addition of the speed difference term allows vehicles to decelerate less aggressively as they approach another vehicle, a stop sign, or a traffic signal. Having computed the vehicle's speed, the vehicle's position is updated every deci-second to reflect the distance that it can travel at this speed during each subsequent deci-second. The updated positions that are derived during each given deci-second then become the basis upon which the new headways and speeds will be computed during the next deci-second. The macroscopic calibration of the microscopic car-following relationship ensures that vehicles will traverse each link in a manner that is consistent with that link's desired free-speed, speed-at-capacity, capacity, and jam density.

A natural byproduct of the above car-following logic is that INTEGRATION represents all queues as horizontal rather than vertical entities. The representation of horizontal queues ensures that queues spill back

upstream, either along a given link or potentially across multiple links. Furthermore, the representation of horizontal queues also ensures that the number of vehicles in the queue will be greater than the net difference between the arrival and departure rate, as the tail of the queue grows upstream towards the oncoming traffic. Finally, the use of the above speed-headway relationship also enables these horizontal queues to exhibit a variable density, depending upon the associated speeds of vehicles within the queue. Research is currently underway to validate the delay, queue size and number of stop estimates computed within the model for isolated signalized intersection approaches.

### **Lane Changing Logic**

When a vehicle travels down a particular link, it may make discretionary lane changes, mandatory lane changes, or both. Discretionary lane changes are a function of the prevailing traffic conditions, while mandatory lane changes are usually a function of the prevailing network geometry.

In order to determine if a discretionary lane change should be made, each vehicle computes three speed alternatives each deci-second. The first alternative represents the potential speed at which the vehicle could continue to travel in its current lane, while the second and third choices represent the potential speeds that this vehicle could travel in the lanes immediately to the left and to the right of its current lane. These speed comparisons are made on the basis of the available headway in each lane and pre-specified biases for vehicles to remain in the lane in which they are already traveling, and to move to the shoulder lane. A vehicle will then elect to try to change into the lane that will permit it to travel at the highest of these three potential speeds.

While discretionary lane changes are made by vehicles in order to maximize their speed, mandatory lane changes arise primarily from a need for vehicles to maintain lane connectivity at the end of each link. In general, lane connectivity requires that eventually every vehicle must be in one of the lanes that is directly connected to the relevant downstream link onto which the vehicle anticipates turning. A unique feature of INTEGRATION's lane-changing model is that the lane connectivity at any diverge or merge is computed internal to the model, saving the model user the extensive amount of hand coding that would be necessary in coding link connectivity in networks with thousands of links.

Once a lane-changing maneuver has been initiated, a subsequent lane change is not permitted until a pre-specified minimum amount of time has elapsed. In the first instance, this minimum ensures that lane changes usually involve a finite length of time to materialize, and that two consecutive lane changes cannot be executed one immediately after the other. Furthermore, while an actual lane-changing maneuver is in progress, the vehicle is modeled as if it partially restricts the headway in the lane it is moving from, and the lane it is changing into. This concurrent presence in two lanes will result in an effective capacity reduction beyond that which would be observed if the vehicle had not made any lane change.

### **Acceleration Constraints**

As mentioned earlier, the INTEGRATION model updates vehicle speeds every deci-second based on the distance headway and speed differential between the subject vehicle and the vehicle immediately ahead of it. Unfortunately, the use of this type of car-following model can result in unrealistically high vehicle accelerations. Consequently, the model also uses a default linear acceleration decay function that results in a reduction in the vehicle's acceleration as a function of its speed. It should be noted that deriving the maximum acceleration from the residual tractive force results in a non-linear function, however a linear relationship does provide a reasonable approximation and is consistent with what was observed in the ORNL data. The INTEGRATION model does provide the user with the opportunity to input the vehicle's power, its weight, the proportion of the total weight on the tractive axle, the frontal area, and the different rolling coefficients to compute the maximum vehicle acceleration more accurately. Finally, it should be noted that within INTEGRATION, vehicles are unable to exceed their maximum acceleration even if they desire to travel at a higher speed based on their car-following model.

## ENERGY AND EMISSION MODELS

### Raw Data Description

The data that were utilized to develop the fuel consumption and emission models were gathered on a dynamometer at the ORNL (West *et al.*, 1997). Given that the focus of this paper is on the development of evaluation tools that are sensitive to vehicle dynamics and not on the ORNL data per se, these data are not described in much detail in this paper. However, these data are described elsewhere in the literature (West *et al.*, 1997). It is sufficient to note that the ORNL data were in the form of look-up tables that included the steady-state fuel consumption and emission rates as a function of the vehicle's instantaneous speed and acceleration. The emission data included hydrocarbon (HC), carbon monoxide (CO), and oxides of nitrogen (NO<sub>x</sub>) emissions. A total of eight light duty vehicles of various weights and engine sizes were utilized (West *et al.*, 1997). West *et al.* indicate that these eight vehicles are representative of current internal combustion (IC) engine technology, as demonstrated in Table 1. Specifically, the average engine size for all vehicles is 3.3 liters, the average number of cylinders is 5.8, and the average curb weight is 1497 kg (3300 lbs; West *et al.*, 1997). Industry reports show that the average sales-weighted domestic engine size for 1995 was 3.5 liters, with an average of 5.8 cylinders (Ward's Automotive Yearbook, 1996; Ward's Automotive Reports, 1995).

The fuel consumption and emission rates were provided for a range of speeds from 0 to 120 km/h (75 mph) at increments of 1.1 km/h (0.69 mph) and for a range of accelerations from  $-1.5 \text{ m/s}^2$  ( $-5 \text{ ft/s}^2$ ) to  $3.6 \text{ m/s}^2$  ( $12 \text{ ft/s}^2$ ) at increments of  $0.3 \text{ m/s}^2$  ( $1 \text{ ft/s}^2$ ). These data included typical driving conditions that ranged from decelerating (acceleration less than zero) to idling (acceleration and speed equal to zero) to acceleration (acceleration greater than zero). Some of the speed/acceleration combinations were unachievable by the vehicles (e.g. high accelerations at high speeds). In general the number of data points ranged from 1300 to 1600 depending on the power of the vehicle (maximum number of potential points was 1980 points [110 speed bins  $\times$  18 acceleration bins]).

Utilizing the data for the eight vehicles, composite fuel consumption and emission surfaces were derived by averaging across the eight vehicles (West *et al.*, 1997). The composite vehicle fuel consumption data varied fairly linearly when the vehicle was cruising or decelerating, however, the relationship was significantly non-linear for higher levels of acceleration (acceleration greater than or equal to  $1.2 \text{ m/s}^2$ ), as illustrated in Figure 1. In terms of emissions, the HC and CO surfaces appeared to be very similar except for the fact that CO emissions were much higher (up to 2500 mg/s in the case of CO versus 60 mg/s in the case of HC). The NO<sub>x</sub> surface appeared to be more non-linear than the HC and CO surfaces when the vehicle was decelerating or cruising.

The authors are aware that the ORNL data that were utilized in developing these models are limited (only 8 vehicles), and do not account for cold starts and high emitters. Furthermore, these data were collected under hot stabilized conditions and as a result may not adequately represent transient catalytic conversion behavior (EPA, 1995), however the ORNL data were the only energy and emission data that were available for third party usage at the time of the study. The Authors are currently utilizing EPA data (100 vehicles) and will be utilizing the University of California, Riverside data (over 300 vehicles) to enhance these statistical energy and emission models (Barth *et al.*, 1997). Furthermore, the authors are also adding the capability to model high emitter and cold start effects on energy and emission estimates.

The focus of this paper is to demonstrate an approach that can be utilized to evaluate energy and emission impacts of operational-level traffic improvement projects. The authors realize that enhancements to the current energy and emission models are required.

## Regression Models

This section briefly describes why and how some regression models were fit to the ORNL data. A detailed description of the various models that were developed is beyond the scope of this paper. Instead, these models, which include different forms of multi-variable non-linear regression models in addition to Artificial Neural Network (ANN) models, are described elsewhere (Ahn *et. al.*, 1999). Ahn *et. al.* (1999) also describe how these models were validated against the ORNL estimates and against MOBILE5. Further research is currently underway to validate these models against EPA second-by-second field measurements for over 100 vehicles. These results will be published shortly.

Fuel consumption and emission regression models were required for two main reasons. First, the regression models were required in order to reduce the data storage requirements of the models. Specifically, the ORNL data set included in the range of 1600 fuel consumption estimates for each vehicle in addition to approximately 1600 observations for each of the emissions. These regression models that are described in this section reduced the storage requirements for each vehicle/MOE combination from up to 1600 parameters to only 16 parameters thus producing major savings in terms of storage requirements. These storage savings are further illustrated if one considers modeling each of the eight vehicles separately (512 versus 51,200 parameters [8 vehicles  $\times$  4 MOE's  $\times$  1600 data points]). The second reason for performing regression analysis is to provide an average estimate of the MOE rates instead of using single observations that are provided by the ORNL data.

Although the details of the regression models are not described in this paper, it is sufficient to note at this point that the basic form of the model is a multi-variable (independent variables were speed and acceleration), non-linear (third degree) model, as demonstrated in Equation (1). Regression models were fit to the raw data in the logarithm space in order to ensure that the regression models did not result in any negative MOE estimates.

$$\log Z_k = \sum_{i=0}^3 \sum_{j=0}^3 B_{ij}^k \times u^i \times a^j \quad \forall k \quad [1]$$

where:

$Z_k$  = Measure of Effectiveness  $k$  (e.g.  $Z_1$ = fuel consumption and  $Z_2$ = HC emissions)

$B_{ij}^k$  = Constant for speed degree  $i$ , acceleration degree  $j$ , and MOE  $k$  (e.g.  $B_{12}^3$  = CO constant for term  $ua^2$ )

$u$  = Vehicle speed

$a$  = Vehicle acceleration

The coefficient of correlation between the raw data and regression fits for each of the four MOEs exceeded 0.90. Figure 1 illustrates some sample fits for the composite vehicle (average of all eight vehicles). The figure demonstrates that the fuel consumption regression fits follow the ORNL data very closely. The emission models do not fit the ORNL data as efficiently (especially for higher levels of acceleration) as is the case for the fuel consumption data, however, the validation of the emission models did indicate that the error relative to using the raw ORNL data was minor (on average within 1.5 percent for fuel consumption and 10 percent for CO emissions) (Ahn *et. al.*, 1999).

## Maximum Acceleration Constraints

It is evident from Figure 1 that the field observations do not extend to higher speed regimes at higher levels of acceleration. For example, at an acceleration of 0 m/s<sup>2</sup>, the data extends to a speed of 120 km/h, while it only extends to 115 km/h when the acceleration is 0.9 m/s<sup>2</sup>, and is further reduced to 60 km/h at an acceleration of 1.8 m/s<sup>2</sup>.

In order to identify the relationship between maximum acceleration and vehicle speed, a number of regression fits were made. Figure 2 illustrates a sample fit where the maximum observed acceleration linearly decreased from  $3 \text{ m/s}^2$  at a speed of 33 km/h to  $1 \text{ m/s}^2$  at a speed of 109 km/h for the composite vehicle. Noteworthy is the fact that for speeds less than 33 km/h the maximum acceleration was not constrained by the vehicle power but was limited by the maximum acceleration that was tested ( $3.6 \text{ m/s}^2$ ). The maximum acceleration regression models resulted in a coefficient of correlation that exceeded 0.95 for all eight vehicles and the composite vehicle. Consequently, the use of a linear acceleration decay function within the INTEGRATION model appears to be consistent with the ORNL data. The linear decay in maximum acceleration results from a reduction in the available tractive force as a function of speed if one assumes a constant vehicle power ( $\text{power}=\text{force}\times\text{speed}$ ). While the relationship is not linear, a linear function does provide a reasonable approximation. A more detailed discussion of the maximum acceleration relationship is beyond the scope of this paper, however it should be noted that a forthcoming publication develops and describes how the maximum acceleration function can be derived from the vehicle power.

It is important to note that the energy and emission models that were developed using the ORNL data are only valid for conditions that were observed in the raw data. Unrealistic results can be obtained if these models are used for data outside the feasible range. Consequently, the ORNL feasible speed/acceleration domain is utilized to constrain vehicle accelerations within the INTEGRATION model.

### **DEMONSTRATION ASSESSMENT OF TRAFFIC SIGNAL CONTROL IMPACTS ON ENERGY AND EMISSIONS**

The energy and emission models that were described earlier were incorporated within the INTEGRATION model as subroutines. Every second, the INTEGRATION model provides the vehicle's instantaneous speed and acceleration to the energy and emission subroutines, which in turn compute the vehicle's fuel consumption and emissions over the previous second. The model accumulates these MOEs across all the vehicles that traverse a specific link in addition to accumulating the MOEs across all the vehicles that travel between two O-D pairs. Summary statistics are provided on a vehicle, link, and O-D basis. Details of how vehicles are generated and the specifics of the INTEGRATION model can be found elsewhere (Van Aerde & Assoc., 1999). It should be noted that the simulation runs only required a couple of minutes to complete given that they did not involve the simulation of a large demand.

Incorporating the previously described energy and emission models within the INTEGRATION traffic assignment and simulation model provides a unique evaluation tool that can be utilized to evaluate alternative ITS and non-ITS applications. This section describes a sample application of the evaluation tool to a traffic-signalized network. A more comprehensive and realistic application in which simulated vehicle speed profiles, energy and emission estimates were compared to estimates that were computed using second-by-second GPS speed measurements along a signalized arterial are provided elsewhere (Rakha *et. al.*, 2000).

The objective of the comparison presented in this paper is to demonstrate that the two main building blocks (vehicle dynamics plus energy and emissions) together produce valid fuel consumption and emission estimates, using systematic simple scenarios. The order in which the scenarios were set up was such that the tool could be evaluated for various levels of sophistication, ranging from simple constant speed scenarios to more sophisticated types of adaptive traffic signal control scenarios. Specifically, the initial set of scenarios involves simulating a single vehicle driving at a constant speed in order to demonstrate the validity of the approach under steady-state conditions. The objective of this scenario is twofold. First, it validates the energy and emission models that were incorporated within the INTEGRATION model when the vehicle is cruising. Second, it validates the simulated vehicle speed profile when the vehicle does not interact with other vehicles.

In the second set of scenarios, various levels of sophistication are introduced to the first scenario. These include variable speeds along a trip and engaging in a number of complete stops. The objective of the second set of scenarios is to quantify the increase in fuel consumption and emissions as a result of vehicle accelerations. The final scenario involves the interaction of vehicles with one another and with traffic controls. The objective of this scenario is to demonstrate the validity of the combined energy/emission model and vehicle dynamics model for typical traffic-operational applications.

In all the scenarios that are presented, a composite vehicle (average across the eight light duty vehicles) was modeled. This composite vehicle represents a typical efficient light duty vehicle (no high emitters included). Furthermore, the fuel consumption and emission estimates that are computed only represent hot stabilized emissions. Further research is currently underway to validate the models against second-by-second field measurements of tailpipe emissions.

### Constant Speed Scenario

The first step in the evaluation exercise was to validate how the combined vehicle dynamics and energy and emission models operated for a number of simple constant speed scenarios. These constant speed scenarios represent artificial scenarios given that they do not involve any vehicle accelerations or decelerations.

The network that was utilized in the analysis was a four-kilometer arterial section. The network was simulated within the INTEGRATION model as four one-kilometer links in order to allow the same network to be utilized for the remainder scenario runs that are described in this paper, as illustrated in Figure 3.

Within the constant speed scenario, a series of sub-scenarios were evaluated in which the free-speed was varied from 25 km/h to 100 km/h at 25 km/h increments (Scenarios 1a through 1d). The objective of Scenarios 1a through 1d was two-fold. First, these scenarios validate the use of a combined vehicle dynamic/energy and emission model under constant speeds (no deceleration/acceleration). Second, these scenarios develop relationships between the steady-state speed and the various MOEs.

As described earlier, the analysis was conducted by simulating a single vehicle that traveled from origin 1 to destination 2. The fuel consumption and vehicle emissions were recorded every second based on the vehicle's instantaneous steady-state speed and acceleration. Because only a single vehicle was simulated on the network, the vehicle traveled at free-speed.

Figure 4 illustrates how the instantaneous speed and acceleration of the vehicle varied as it traveled through the network. It is evident from the figure that the vehicle entered the network after 30 seconds of simulation at free-speed (25 km/h for Scenario 1a). Because the vehicle traveled at constant speed, the acceleration remained at 0 m/s<sup>2</sup> for the entire trip. The fuel consumption rate remained constant at approximately 0.001 liters/second (3.6 liters/hour). This fuel consumption rate of 3.6 liters/hour is consistent with the data that were obtained from ORNL for a constant speed of 25 km/h (Figure 1). Figure 4 illustrates that the CO emission rates were approximately ten-fold higher than the HC and NO<sub>x</sub> emission rates (10 versus 1 mg/s). These findings are consistent with the raw data that were obtained from the ORNL, as illustrated in Figure 5. Although the fit for the CO regression model might not appear accurate at high speeds, it should be noted that a comparison of the emission estimates for a number of driving cycles indicated that the error was within 10 percent on average (Ahn *et. al.*, 1999).

Figure 6 illustrates the impact of various constant speeds on the fuel consumption along the four-kilometer trip. The fuel consumption varies from a maximum of 0.53 liters (at a constant speed of 25 km/h) to a minimum of 0.35 liters (at a constant speed of 75 km/h). The fuel consumption function, together with the fuel consumption rates, is consistent with the raw data that were obtained from ORNL. Figure 6 illustrates that CO emissions are considerably higher than the HC and NO<sub>x</sub> emissions. Furthermore, the difference increases with the increase in the vehicle speed (difference of 5 grams at a speed of 25 km/h versus a difference of 10 grams at a speed of 100 km/h). The HC relationship indicates that the optimum speed in terms of HC emissions is 50 km/h, while the CO and NO<sub>x</sub> relationships indicate that the vehicle emissions

increase with an increase in vehicle speed (optimum located at minimum speed that is 25 km/h). It is evident from the figure that the CO emissions are more sensitive to the vehicle speed.

### Variable Speed Scenario

The next scenario to be evaluated was a variable speed scenario (Scenario 2). In the variable speed scenario, the free-speed on links 1 and 3 was set at 25 km/h, and on links 2 and 4 was set at 75 km/h. Again, a single vehicle was simulated to travel between origin 1 and destination 2.

Figure 7 illustrates the temporal variation in vehicle speed and acceleration as the vehicle traversed the test network. Figure 7 demonstrates that the vehicle required approximately 10 seconds to accelerate from a speed of 25 km/h to a speed of 75 km/h (average acceleration rate of  $1.4 \text{ m/s}^2$ ). Furthermore, the figure illustrates that the vehicle acceleration decreased as the vehicle speed increased, as was demonstrated earlier in Figure 2 (decreased from 1.2 to  $0.8 \text{ m/s}^2$  which corresponds to an acceleration rate equivalent to 0.5 the maximum acceleration rate).

Figure 7 also illustrates a seven-fold increase in the fuel consumption rate when the vehicle accelerated at a rate of  $1 \text{ m/s}^2$  at a speed of 60 km/h versus cruising at a speed of 25 km/h. Furthermore, one can observe a two-fold increase in the instantaneous fuel consumption rate for a cruising speed of 75 km/h versus 25 km/h. Consequently, Figure 7 demonstrates that the combination of vehicle acceleration and speed significantly impacts vehicle fuel consumption and emission estimates. The combined impact of vehicle acceleration and speed is more evident for the HC emission estimates where the emissions do not increase significantly until the vehicle has attained a speed of approximately 50 km/h although the acceleration level is higher at the lower speeds.

The impact of vehicle accelerations on the fuel consumption is also evident from Figure 6, which illustrates that the fuel consumed by a vehicle with a constant average speed of 37 km/h is lower than that experienced by the same vehicle if the average speed involves some level of acceleration and deceleration (0.5 versus 0.6 liters of fuel consumed). Similar results were found for the vehicle emissions. Specifically, vehicle emissions of HC were less for a constant speed (0.4 versus 1.1 grams), CO emissions were considerably less (6.3 versus 23.0 grams), and  $\text{NO}_x$  emissions were also less (0.7 versus 1.7 grams).

### Stop Sign Scenario

In the next scenario, three stop signs were simulated which were located at nodes 10, 11, and 12, respectively. These stop signs required the approaching vehicle to make a complete stop before accelerating to its free-speed, as illustrated in Figure 8. Again, as was the case in Scenario 1, Scenario 3 involved four sub-scenarios in which the vehicle free-speed varied from 25 to 100 km/h at 25 km/h increments (labeled as Scenarios 3a through 3d).

Figure 8 demonstrates that the vehicle did not decelerate in excess of  $1 \text{ m/s}^2$  when it approached the stop sign. Furthermore, the figure illustrates a decay in the level of acceleration as the vehicle speed increased. Finally, Figure 8 also demonstrates an increase in the instantaneous CO emissions as the vehicle accelerated to its free-speed. Currently, the INTEGRATION model assumes acceleration rates that do not exceed 50 percent the maximum acceleration rate based on a preliminary analysis of GPS data collected along an arterial corridor. Alternatively, an EPA (1993b) study indicated that typical acceleration rates were in the range of 20 percent the maximum level, however it is not clear if these acceleration rates were constrained by the vehicle driver or by the surrounding traffic. Consequently, further research is required in order to quantify typical driver acceleration rates under differing levels of congestion for usage within a microscopic simulation environment.

Figure 9 illustrates how the simulated speed profile of a vehicle approaching a stop sign varies as a function of the vehicle's approach speed. Specifically, Figure 9 demonstrates that the vehicle starts decelerating 400 meters upstream from the stop sign when the vehicle approach speed is 100 km/h. The figure also

demonstrates that once the vehicle has decelerated to a speed of 50 km/h, its speed profile becomes very similar to the speed profile of a vehicle approaching the stop sign at a speed of 50 km/h. The speed profiles coincide at the lower speeds because the vehicle attempts to maintain a constant level of deceleration. The figure also demonstrates similar speed profiles downstream of the stop sign.

Figure 9 also illustrates a sample simulated and field observed speed profile along the Scottsdale/Rural Road corridor in Phoenix. Figure 9 demonstrates that the simulated deceleration and acceleration profile is consistent with second-by-second GPS speed measurements. Specifically, the simulated and field vehicle starts decelerating approximately 200 meters upstream the stop sign. Further research is currently underway to compare simulated and field speed and acceleration estimates for differing approach speeds and levels of aggressiveness.

Figure 10 illustrates that the delay experienced by a vehicle approaching a series of stop signs increases as the approach speed increases. The increase in delay as a function of approach speed is a result of the larger amount of time involved in decelerating/accelerating for higher speed differentials. The fuel consumption rates also increase with the increase in speed differential, with the optimum speed shifting from 75 km/h (in the case of no stops) to 50 km/h (in the case of 3 stops). The HC emissions experience a similar uneven shift in the function (larger increase for higher speeds). These results demonstrate the difficulty in predicting the emission impacts of simple traffic control scenarios.

### **Traffic Signal Coordination Scenario**

The final evaluation exercise involved modeling three equally spaced traffic signals along the same arterial section (signals located at nodes 10, 11, and 12). The spacing of the traffic signals was set at 0.35 km (reducing the spacing between nodes 10, 11, and 12) in order to minimize any platoon dispersion that could occur when vehicles leave a traffic signal. Three types of traffic signal control were considered. The first of these traffic signal control scenarios involved bad off-line signal coordination, while the second involved good off-line signal coordination, and the third involved a form of adaptive signal coordination.

Figure 11 illustrates the time/space diagram for the three types of traffic signal control that were evaluated. It is evident from Figure 11 that the vehicles have to make a stop at each of the three traffic signals in the case of bad signal coordination (Case a), while in the case of implementing a good off-line plan, vehicles have to make a single stop at the first traffic signal and then proceed downstream without making any further stops (Case b). Finally, a form of adaptive coordinated control that is implemented within the INTEGRATION model was utilized to optimize the offsets of the traffic signals. Figure 11 illustrates how the optimizer initially optimizes the offset of Signal 2 that is completely optimized after four-cycle lengths, while the offset of Signal 3 is optimized after six cycle lengths. Finally, the adaptive algorithm converges to the optimum signal timings after six cycle lengths.

Figure 12 illustrates the impact of various levels of traffic signal control on vehicle delay, fuel consumption, and emissions. While this is a very simple example, Figure 12 demonstrates that depending on the level of traffic signal coordination, traffic signal coordination can result in significant reductions in delay. Furthermore, the level in traffic signal coordination can result in major reductions in fuel consumption and vehicle emissions (in the range of 50 percent). It must be noted here that these results are specific to the network and traffic characteristics that were modeled. Specifically, only through-traffic in a single direction was modeled. If cross-street demands were considered in addition to traffic in either direction along the major arterial, the benefits would be less significant. However, the three signalized cases that were described do demonstrate the feasibility of utilizing the INTEGRATION model to not only evaluate alternative types of traffic signal control, but also to optimize the traffic signal timings.

### APPLICATION OF MODEL TO FIELD DATA

The objective of this section is to demonstrate that the microscopic energy and emission model, which requires speed and acceleration measurements as input, can run on either simulated or field data. Consequently, the microscopic energy and emission model was applied to field speed and acceleration data that were gathered using GPS-equipped vehicles. The GPS data were gathered along a 10-km section of a signalized arterial in Phoenix, Arizona (Scottsdale/Rural Road from Thomas Road in the North to Southern Road in the South) (Rakha *et. al.*, 2000). Speeds were computed utilizing the Doppler technique, which measures the instantaneous shift in the GPS satellite signal at that instant, while vehicle accelerations were computed from the speed measurements. Robust smoothing techniques were required to eliminate unrealistic acceleration estimates. A forthcoming paper will describe how these techniques were applied to the GPS data.

Figure 13 illustrates how the speed and acceleration profile varies as a vehicle traverses the 10-km section. It is evident from the speed profile that the vehicle makes a number of partial and complete stops along the section. The acceleration profile indicates a considerable amount of noise. The acceleration profile also illustrates that vehicle rarely accelerated at rates in excess of  $3.6 \text{ m/s}^2$ , which is the maximum rate considered in the ORNL data (1 observation out of approximately 1000 observations). These unrealistic acceleration estimates were eliminated through a form of robust data smoothing, as indicated earlier. Figure 13 illustrates the fuel consumption estimates that result after applying the fuel consumption model to the field speed and acceleration estimates. Comparing Figure 7 to Figure 13 it appears that the fuel consumption estimates using field and simulation data are fairly consistent in absolute terms ranging from 0.5 milliliters/second to 7 milliliters/second. A more detailed description of the field and simulation comparison is provided elsewhere (Rakha *et. al.*, 2000).

### CONCLUSIONS OF STUDY AND RECOMMENDATIONS FOR FURTHER WORK

The study demonstrated that the microscopic energy and emission model could be applied to both simulated and field speed and acceleration measurements. Furthermore, this paper has demonstrated how the combined use of a microscopic vehicle dynamic model, together with a microscopic vehicle energy and emission model, can be utilized to evaluate alternative ITS and non-ITS applications. Specifically, microscopic energy and emission models were incorporated within the INTEGRATION traffic assignment and simulation model to provide a unique evaluation tool. As a test of feasibility, this tool was utilized to evaluate alternative types of traffic control.

The study demonstrated that for steady-state conditions (no vehicle accelerations), the tool predicted vehicle fuel consumption and emissions consistently with field data that were obtained from ORNL. Furthermore, the study demonstrated that vehicle fuel consumption and emissions are sensitive to the combined level of vehicle acceleration and speed. Furthermore, this study has demonstrated that the use of tools that base their fuel consumption and emission estimates on the average trip speed would fail to capture the impact of a significant factor (vehicle acceleration) on these MOE's.

Further research is required in a number of areas including: modeling traffic diversion and induced traffic demand that result from ITS and non-ITS alternatives, the independent validation of simulated speed and acceleration data, the independent validation of estimated fuel consumption and emission estimates using direct on-road measurements, capturing cold start and temperature effects on vehicle fuel consumption and emissions, and modeling high emitters.

### ACKNOWLEDGMENTS

The authors gratefully acknowledge the support of the Federal Highway Administration and the Environmental Protection Agency to conduct the research described in this paper. Special thanks to Mark

Carter at SAIC, Cecilia Ho at FHWA, Robert Noland at EPA, James Carpenter at EPA, and David Brzezinski at EPA. The authors would also like to thank Brian West and Scott Sluder at ORNL for sharing their fuel consumption and emission data.

## REFERENCES

- Ahn K., Trani A.A., Rakha H.A., Van Aerde M. (1999), "Microscopic Fuel Consumption and Emission Models" Presented at the Transportation Research Board 78<sup>th</sup> Annual Meeting, January.
- Barth M., Younglove T., Wenzel T., Scora G., An F., Ross M., and Norbeck J. (1997), *Analysis of Model Emissions from Diverse In-Use Vehicle Fleet*, Transportation Research Record 1587, pp. 73-84.
- Environmental Protection Agency (EPA) (1993a), *Mobile 5A User Guide*, Ann Arbor, Michigan.
- Environmental Protection Agency (EPA) (1993b), *Federal Test Procedure Review Project: Preliminary Technical Report*, EPA Report 420-R-93-007.
- Rakha H. and M. Van Aerde. (1996). *Comparison of Simulation Modules of TRANSYT and INTEGRATION Models*, Transportation Research Record 1566, pp. 1-7.
- Rakha H., Van Aerde M., Bloomberg L., and Huang X. (1998), *Construction and Calibration of a Large-Scale Micro-Simulation Model of the Salt Lake Area*, Transportation Research Record.
- Rakha H., Medina A., Sin H., Dion F., Van Aerde M., and Jenq J. (2000), "Coordination of Traffic Signals across Jurisdictional Boundaries: Field and Modeling Results," Accepted for Presentation at the Transportation Research Board 79<sup>th</sup> Annual Meeting, January.
- M. Van Aerde & Assoc. (1999), *INTEGRATION Release 2.20 User's Guide*.
- Van Aerde M. and Yagar S. (1988a), *Dynamic Integrated Freeway/Traffic Signal Networks: Problems and Proposed Solutions*, Transportation Research, Vol. 22A, No. 6, pp. 435-443.
- Van Aerde M. and Yagar S. (1988b), *Dynamic Integrated Freeway/Traffic Signal Networks: A Routing-Based Modeling Approach*, Transportation Research, Vol. 22A, No. 6, pp. 445-453.
- Van Aerde M., B. Hellinga, M. Baker, and H. Rakha. (1996), "INTEGRATION: An Overview of Current Simulation Features," Transportation Research Board 75<sup>th</sup> Annual Meeting, Washington, D.C.
- Van Aerde, M. and H. Rakha (1995), "Multivariate Calibration of Single Regime Speed-Flow-Density Relationships," VNIS/Pacific Rim Conference Proceedings, Seattle, WA, pp. 334-341, ISBN 0-7803-2587-7, IEEE 95CH35776.
- Ward's Automotive Yearbook (1996), 58 Edition, Ward's Communications, Southfield, MI, Intertec Publishing.
- Ward's Automotive Reports (1995), Ward's Communications Vol. 70, No. 51, December, Southfield, MI, Intertec Publishing.
- West, B., McGill, R., Hodgson, J., Sluder, S., Smith, D. (1997), "Development of Data-Based Light-Duty Modal Emissions and Fuel consumption Models," Society of Automotive Engineers Paper No. 972910

**Table 1. Test Vehicle and Industry Average Specifications (Source: West, *et al.* 1997)**

Year	Make/Model	Engine	Curb Weight kg (lbs.)	Rated HP kW (HP)	City/Highway EPA Fuel Economy km/L (mpg)
<b><i>Light-Duty Vehicle</i></b>					
1988	Chevrolet Corsica	2.8L Pushrod V6, PFI	1209 (2665)	97 (130)	8/12 (19/29)
1994	Oldsmobile Cutlass Supreme	3.4L DOHC V6, PFI	1492 (3209)	157 (210)	7/11 (17/26)
1994	Oldsmobile Eighty Eight	3.8L Pushrod V6, PFI	1523 (3360)	127 (170)	8/12 (19/29)
1995	Geo Prizm	1.6L OHC I4, PFI	1116 (2460)	78 (105)	11/13 (26/30)
1993	Subaru Legacy	2.2L DOHC Flat I4, PFI	1270 (2800)	97 (130)	9/12 (22/29)
	5-Car Average	2.8L, 5.2 Cylinders	1322 (2915)	111 (149)	
1995	LDV Industry Average	2.9L, 5.4 Cylinders	1315 (2900)		
<b><i>Light Duty Trucks</i></b>					
1994	Mercury Villager Van	3.0L Pushrod V6, PFI	1823 (4020)	113 (151)	7/10 (17/23)
1994	Jeep Grand Cherokee	3.0L Pushrod I6, PFI	1732 (3820)	142 (190)	6/9 (15/20)
1994	Chevrolet Silverado Pickup	5.7L Pushrod V8, TBI	1823 (4020)	149 (200)	6/9 (14/18)
	3-Truck Average	4.2L, 6.7 Cylinders	1793 (3953)	134 (180)	
1995	LDT Industry Average	4.6L, 6.5 Cylinders			
<b><i>Overall Average</i></b>					
	8-Vehicle Average	3.3L, 5.8 Cylinders	1497 (3300)	119 (160)	
1995	Industry Average	3.5L, 5.8 Cylinders			

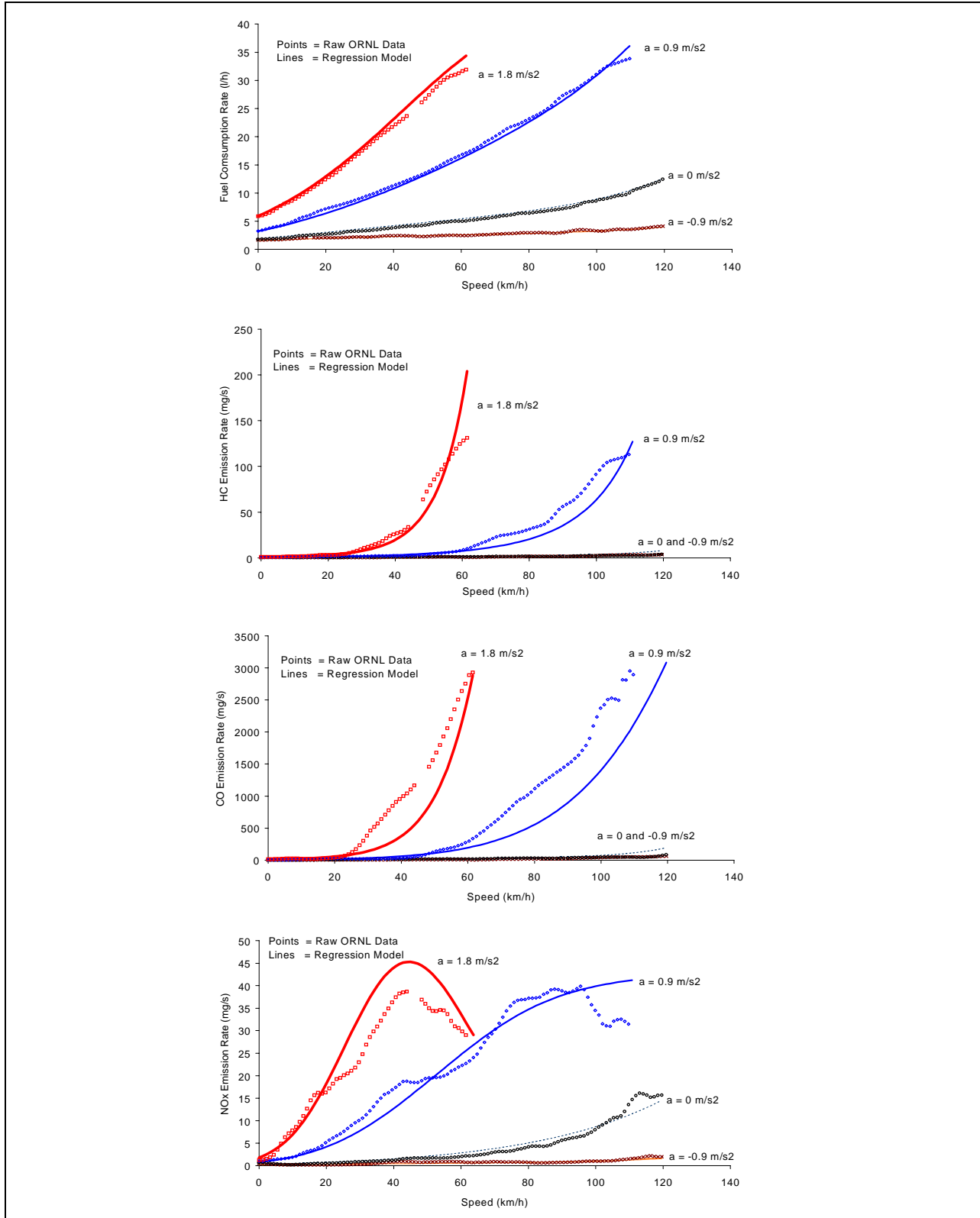
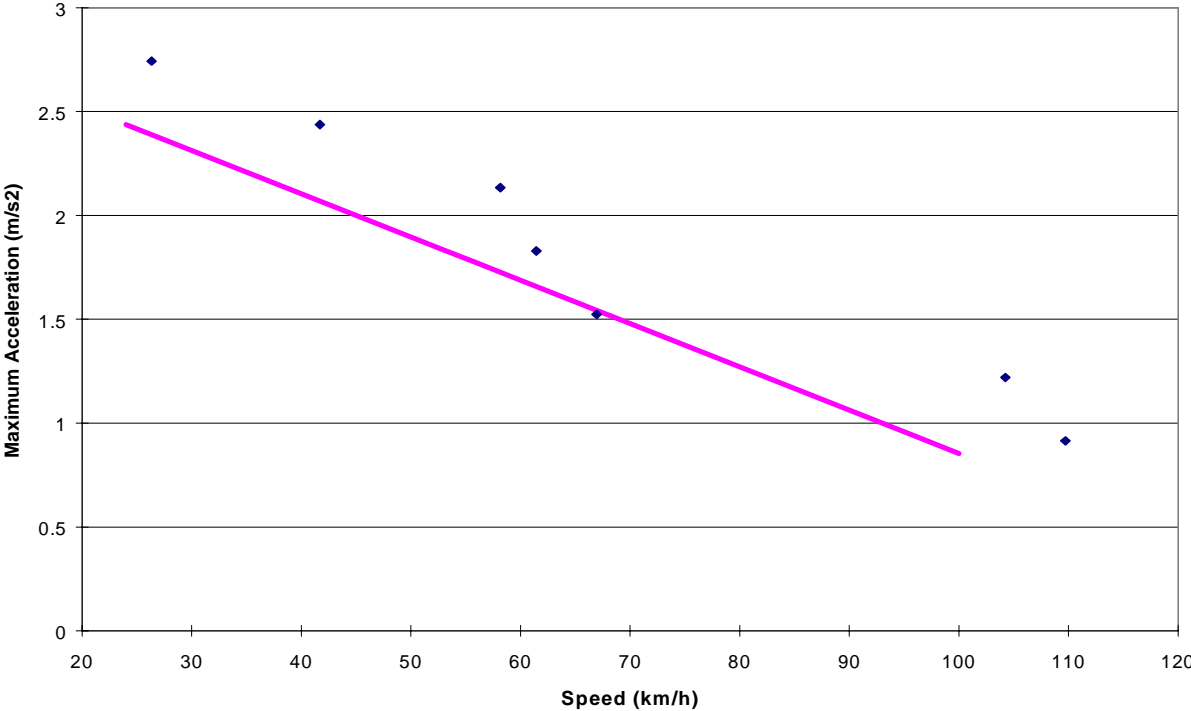


Figure 1. Regression Fit for Fuel Consumption, HC, CO and NO<sub>x</sub> Emissions (Composite Vehicle)



**Figure 2. Maximum Acceleration Capabilities (Composite Vehicle)**



**Figure 3. Network Illustration**

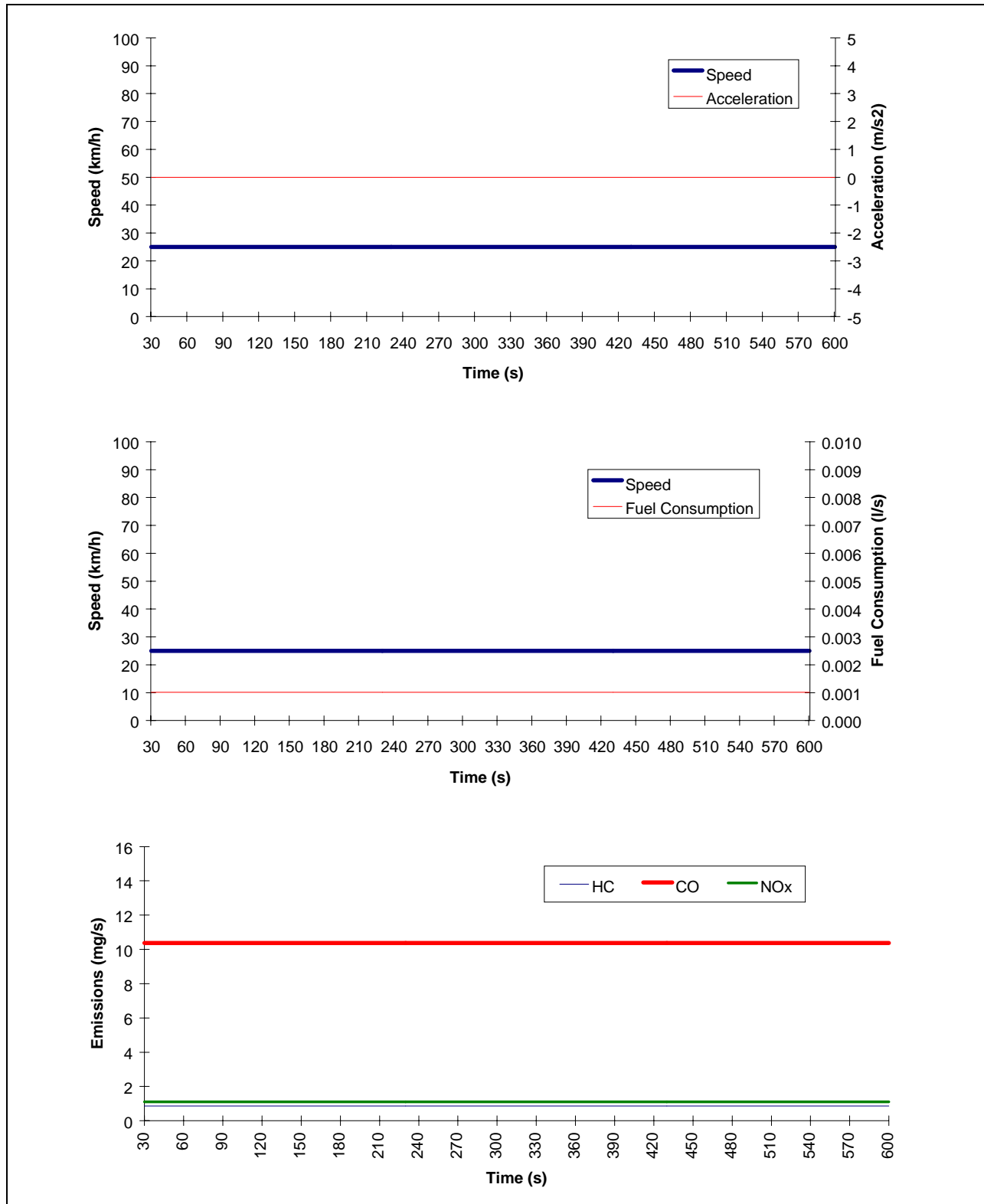


Figure 4. Variation in Instantaneous Fuel Consumption and Emissions for Constant Speed Scenario

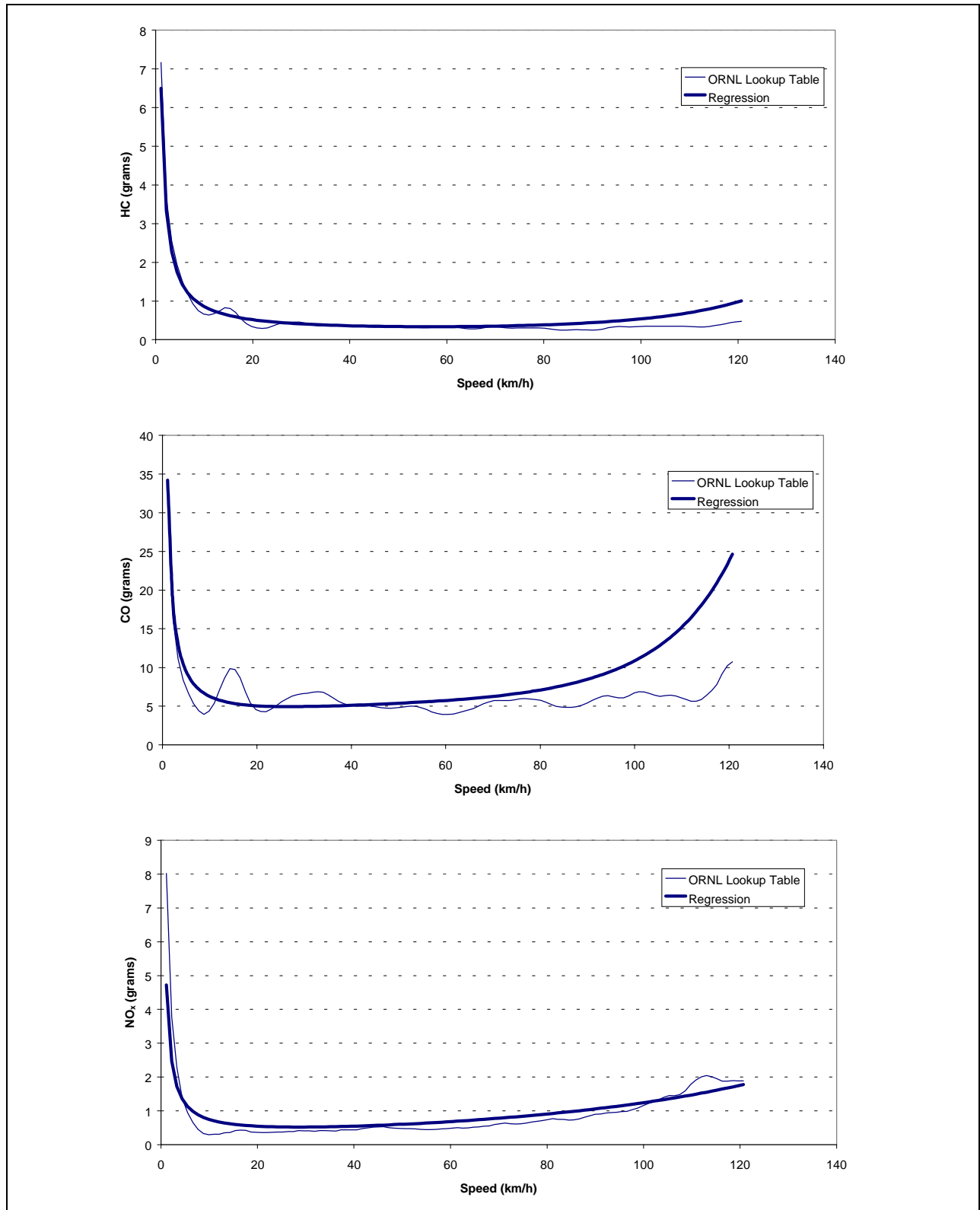


Figure 5. Comparison of ORNL Lookup and Regression Emission Estimates

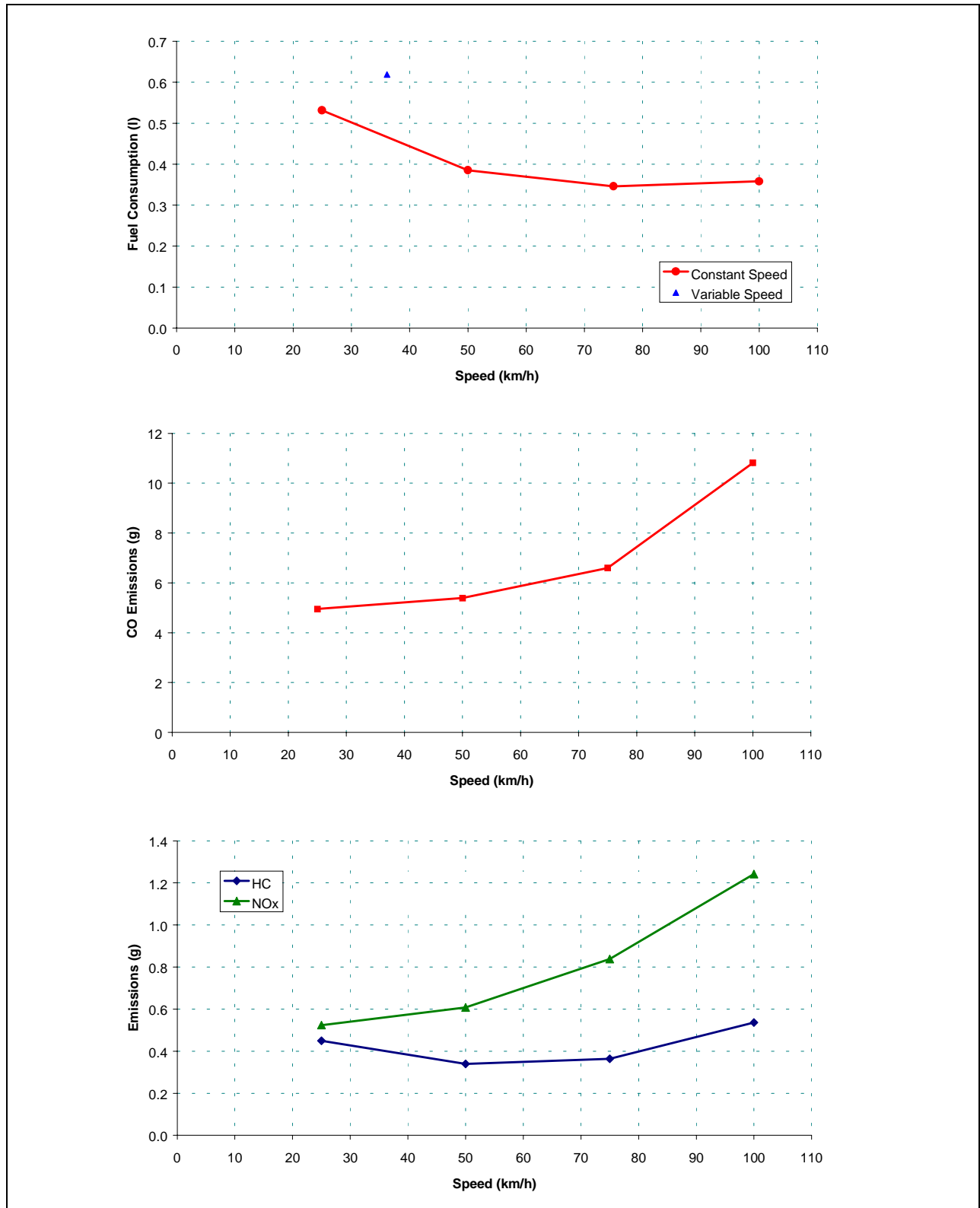
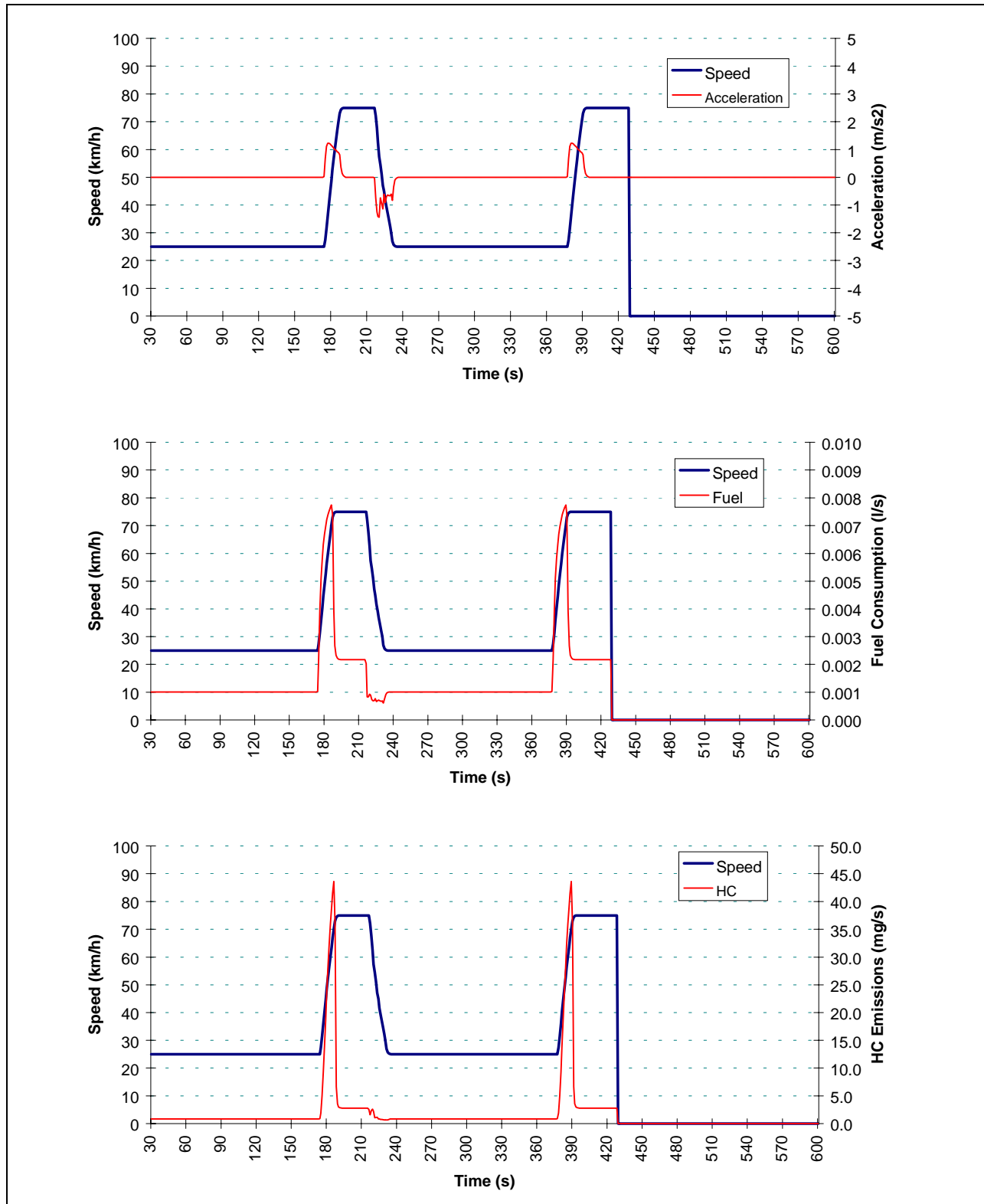


Figure 6. Impact of Constant and Variable Speed on Vehicle Fuel Consumption and Emissions



**Figure 7. Variation in Instantaneous Fuel Consumption and HC Emissions for Variable Speed Scenario**

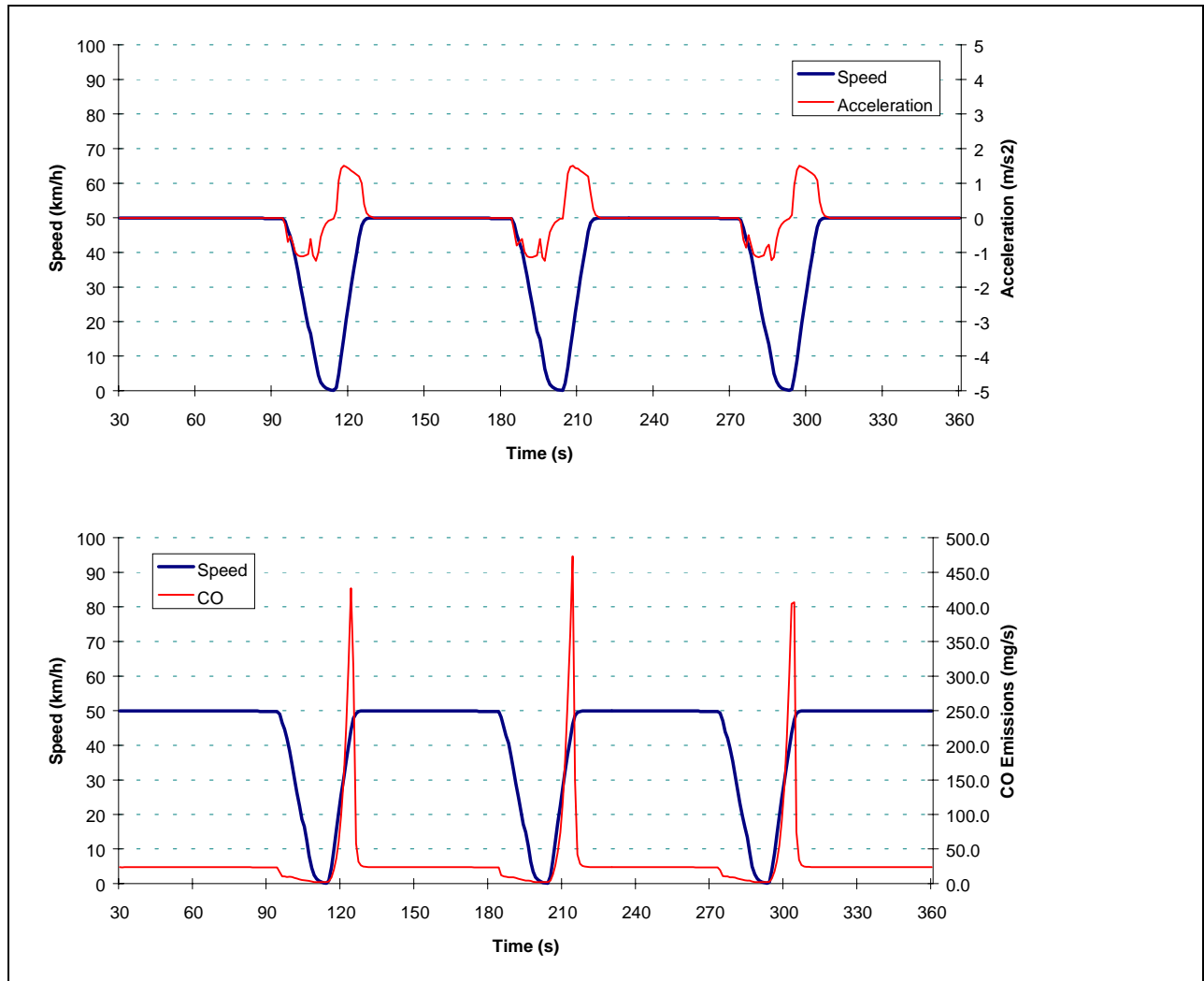


Figure 8. Variation in Instantaneous Fuel Consumption and CO Emissions for Stop Sign Scenario

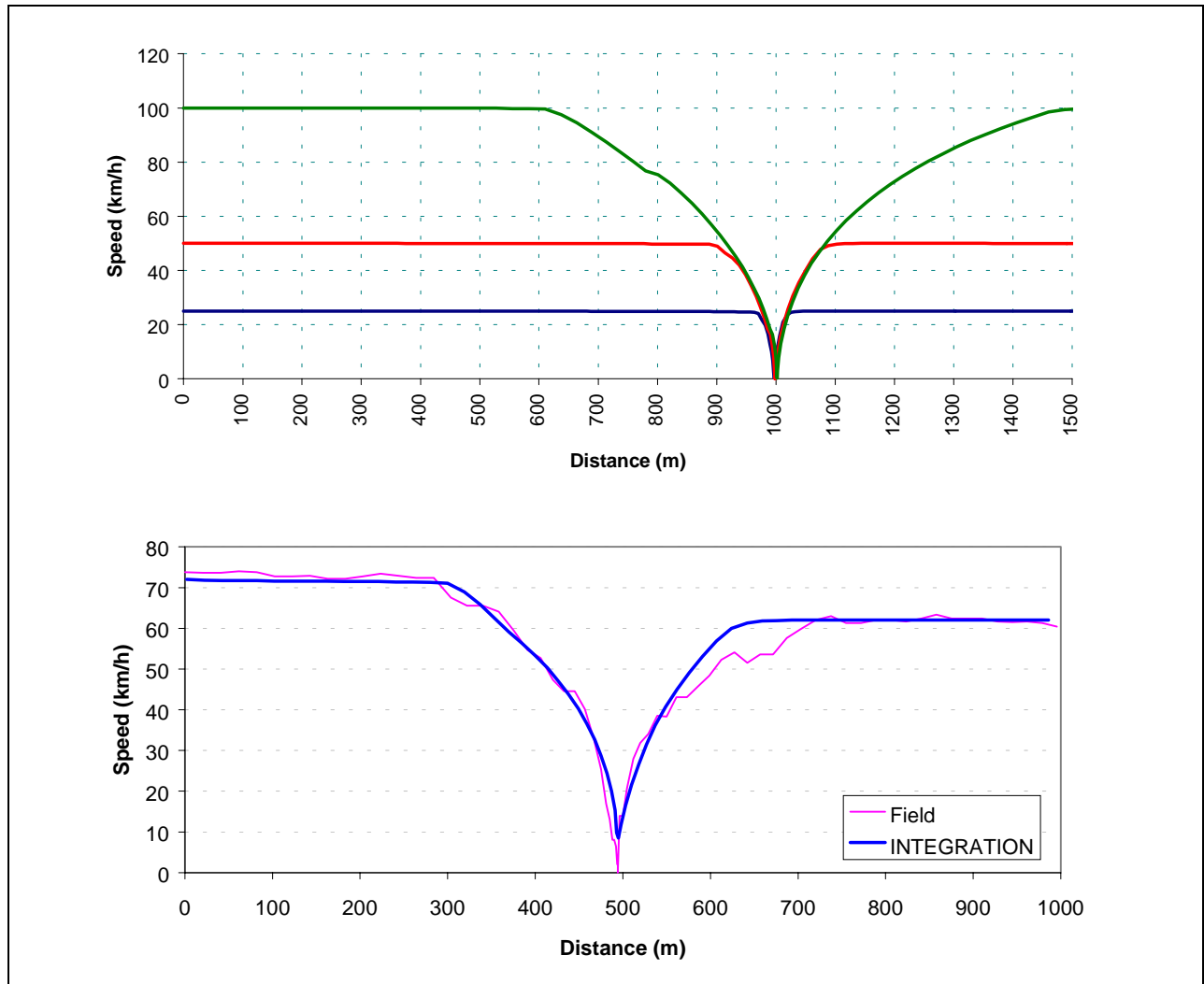
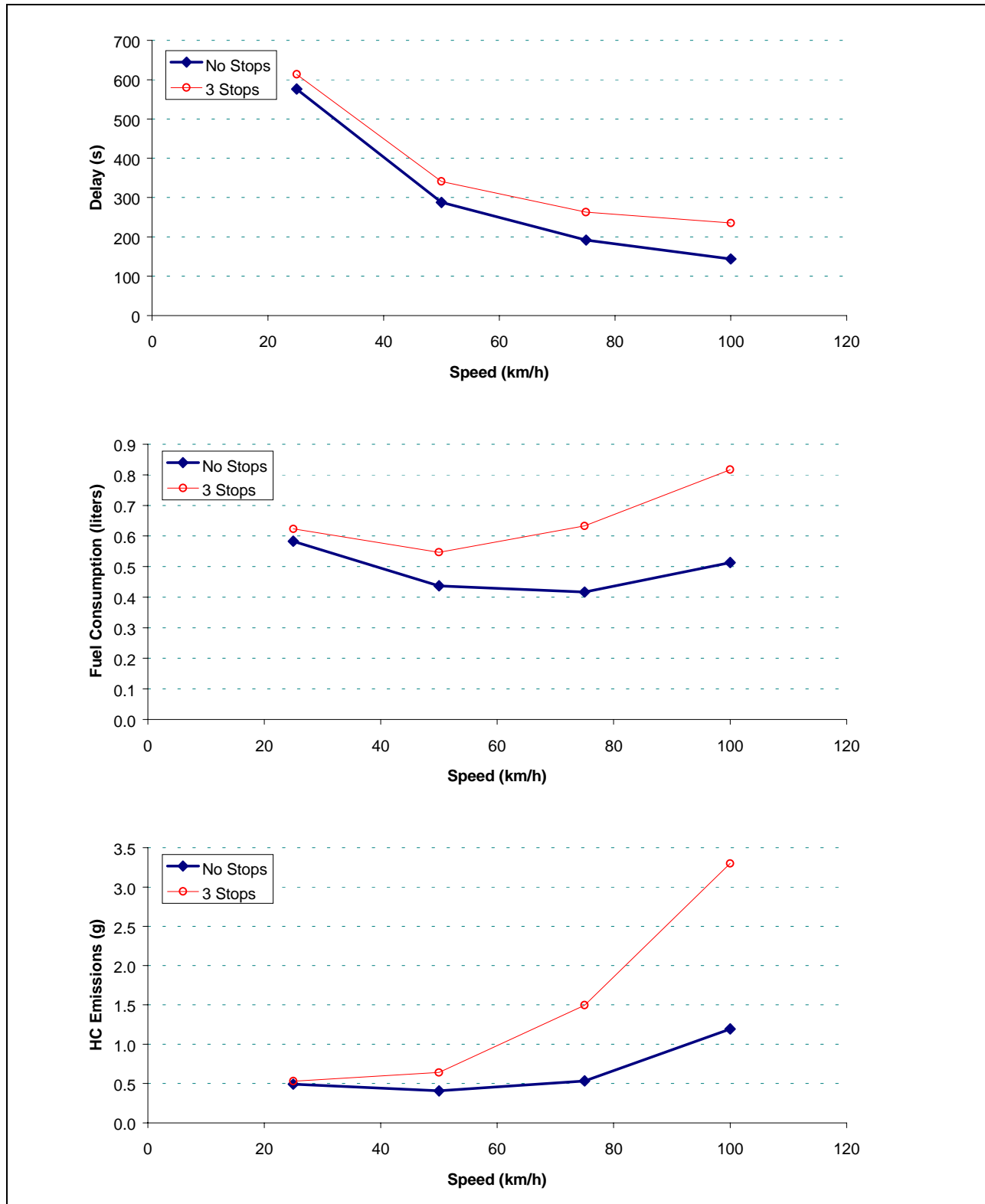


Figure 9. Vehicle Speed Profile Approaching a Stop Sign as a Function of Initial Speed



**Figure 10. Variation in Vehicle Delay, Fuel Consumption, and HC Emissions as a Function of Number of Stops**

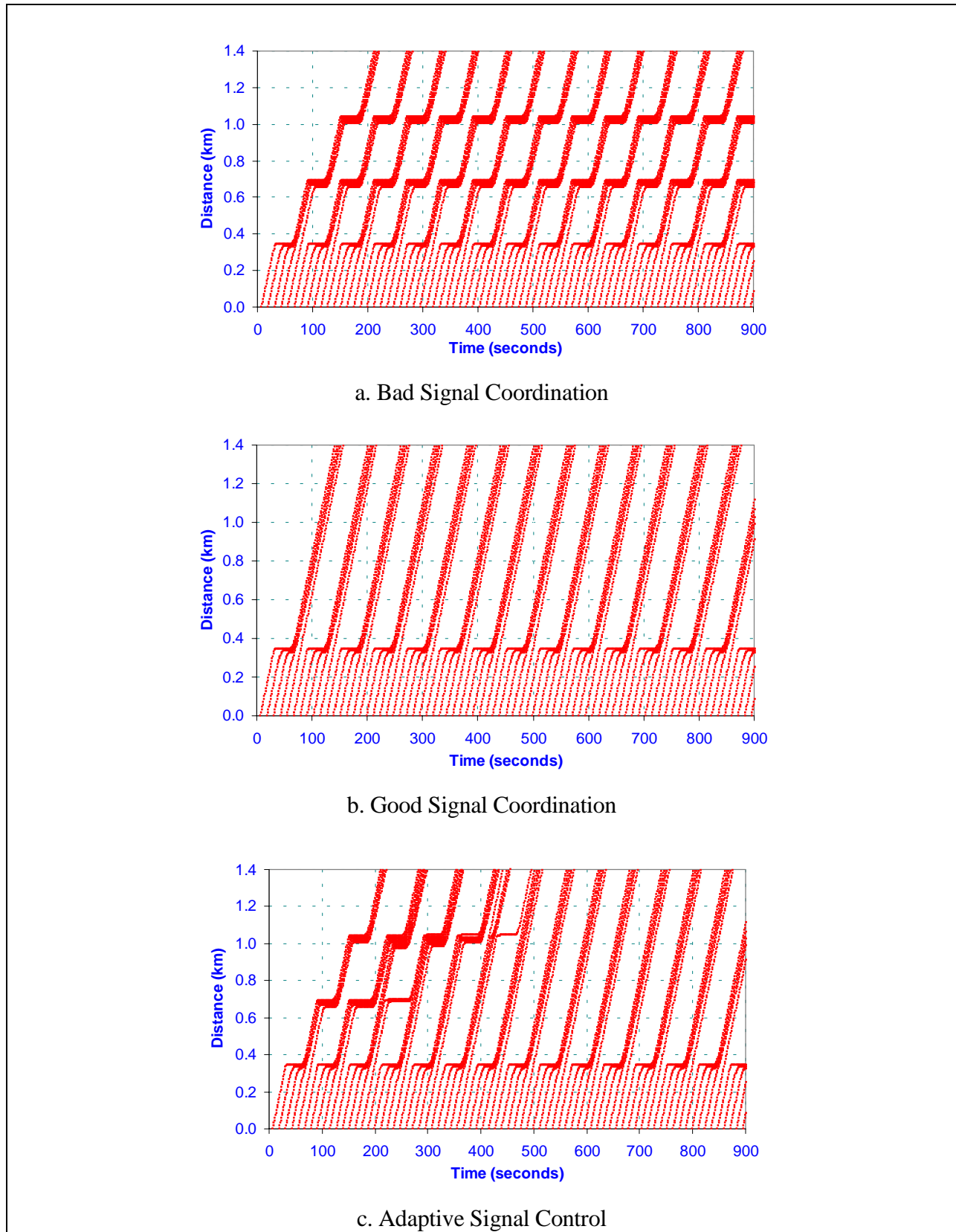
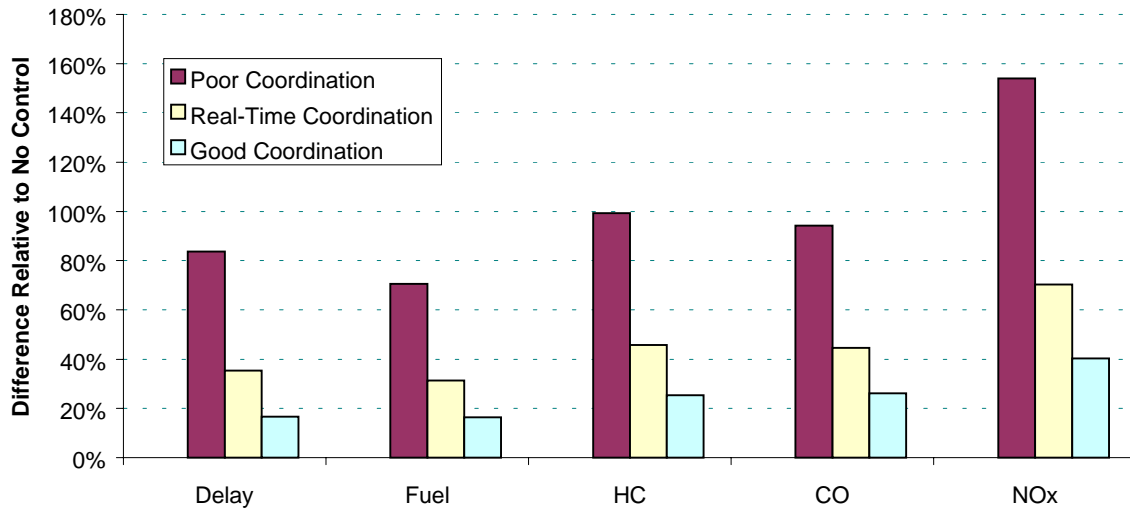


Figure 11. Time/Space Diagram for Various Levels of Signal Optimization



**Figure 12. Impact of Type of Signal Control on Vehicle Delay, Fuel Consumption, and Emissions**

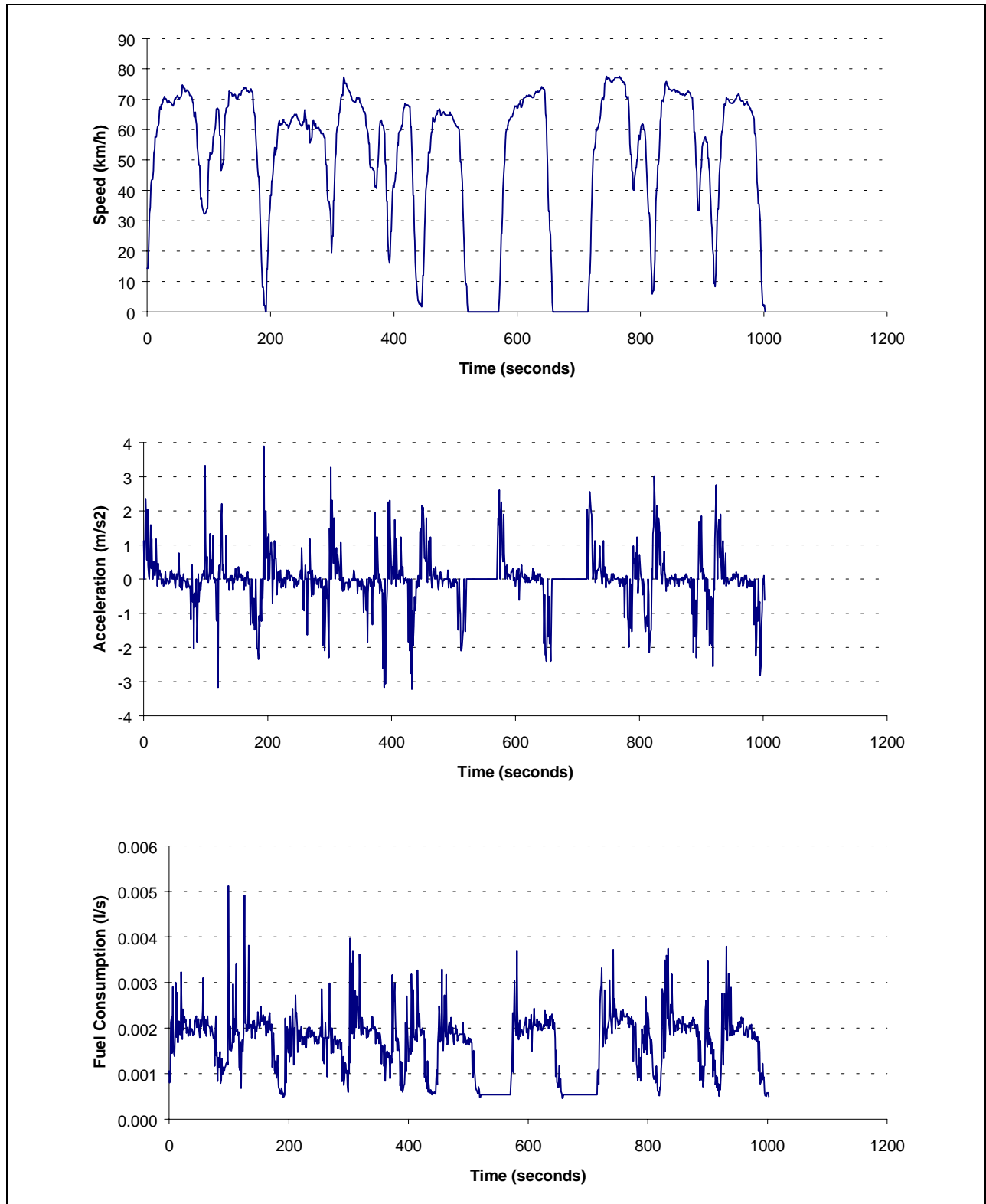


Figure 13: Application of fuel consumption model to field data